Inorganic Chemistry

ARTICLE

pubs.acs.org/IC

Ring-Opening Polymerization of Cyclic Esters and Trimethylene Carbonate Catalyzed by Aluminum Half-Salen Complexes

Donald J. Darensbourg,* Osit Karroonnirun, and Stephanie J. Wilson

Department of Chemistry, Texas A&M University, College Station, Texas 77843, United States

Supporting Information

ABSTRACT: A series of ONO-tridentate Schiff base ligands derived from chiral and achiral amino alcohols and amino acids were synthesized and reacted with $AlEt_3$ to provide dimeric aluminum complexes. These complexes were tested for the ring-opening polymerization (ROP) of *rac*-lactide at 70 °C in toluene, producing poly(lactide) with up to 82% isotacticity. The most active of these aluminum complexes was chosen to perform ring-opening homopolymerizations of *rac*-lactide, trimethylene carbonate (TMC), *rac*-β-butyrolactone (*rac*-β-BL), δ-valerolactone (δ-VL), and ε-caprolactone (ε-CL). Kinetic parameters were investigated, and each polymerization was found to be first order with respect to monomer concentration. Fractional orders were observed with respect to catalyst concentration, indicating catalyst aggregation during the polymerization processes. Activation parameters were determined for all monomers, with their $\Delta G^{\ddagger}$ values at 90 °C being in the order *rac*-lactide ≈ *rac*-β-BL > δ-VL > TMC ≈ ε-CL. Fineman−Ross and kinetic studies of the copolymerization of *rac*-lactide and δ-VL both indicate that the rate of *rac*-lactide enchainment is higher than that of δ-VL, resulting in a tapered copolymer. In addition, single crystals of one of these aluminum complexes were grown in the presence of *rac*-lactide and characterized using X-ray crystallography. The unit cell contains two lactide monomers, one D- and one L-lactide, adding further proof that polymerization takes place via an enantiomorphic site control mechanism.

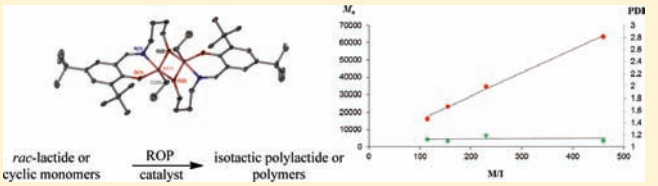

INTRODUCTION

Much research is currently focused on the development of polymers with sophisticated macromolecular structures derived from renewable resources.[1] Among the most well-studied of these nonpetrochemical based polymeric materials are those synthesized from lactides. Polylactides (PLA) which originate from replenishable resources such as corn, wheat, and sugar beets are biodegradable polymers widely used not only in commodity plastics, that is, the textile industry,[2] but also in medical applications such as drug delivery[3] and tissue engineering.[4] On the other hand, polyhydroxybutyrate (PHB) is an aliphatic polyester produced by a variety of microorganisms and bacteria.[5] Hence, PHB can be degraded by microorganisms and used as a source of internal energy and carbon reserve. Importantly, over 300 bacterial species are known to synthesize polyhydroxyalkonoates (PHAs).[6] The mechanical properties of PHB are similar to those of petrochemical-based polymers, allowing PHB to be a potential replacement polymer for the packaging and agricultural industries.[6,7] It is also worthy to note that both PLA and PHA exhibit very good green design assessments as well as moderate life cycle assessments.[8]

Poly-ε-caprolactone (PCL) and poly-δ-valerolactone (PVL) are other examples of biobased aliphatic polyesters that have emerged as important materials in industrial processes that require biodegradable high performance plastics. In addition, PCL, because of various valuable properties of the polymer, finds uses in the construction industry.[9] Polytrimethylene carbonate (PTMC) is a biodegradable polymer which degrades without forming acidic compounds. This property of PTMC makes it ideal for applications involving protein delivery, since low pH conditions tend to lead to protein denaturation.[10] Although these biobased polymers can be employed in numerous applications, a common use of these biodegradable polymers is in drug delivery, for they are readily removed from the human body via normal metabolic pathways.[11]

We have recently demonstrated that aluminum half-salen complexes are effective catalysts for the ring-opening polymerization (ROP) of *rac*-lactide.[12] Herein, we wish to report extensive studies of these catalysts for the ring-opening polymerization of cyclic monomers, *rac*-lactide, trimethylene carbonate (TMC), *rac*-β-butyrolactone (*rac*-β-BL), δ-valerolactone (δ-VL), and ε-caprolactone (ε-CL). Included in these investigations are X-ray structural analysis of the aluminum complexes, kinetic studies for the ROP of various cyclic monomers, as well as kinetic studies of copolymerization reactions of *rac*-lactide and δ-VL.

RESULTS AND DISCUSSION

Synthesis and X-ray Structural Characterization of Aluminum Complexes. As described in our earlier report the aluminum complexes were prepared by treatment of the appropriate Schiff base ligand with a stoichiometric quantity of $AlEt_3$ in dry toluene.[12] Scheme 1 illustrates the synthesis of these dimeric aluminum complexes, along with their designated numeric label, derived from the reaction of triethylaluminum and chiral amino alcohols (**2a**−**d**), aliphatic amino alcohols (**2e**−**i**), and amino

Received: April 21, 2011
Published: June 15, 2011

Scheme 1

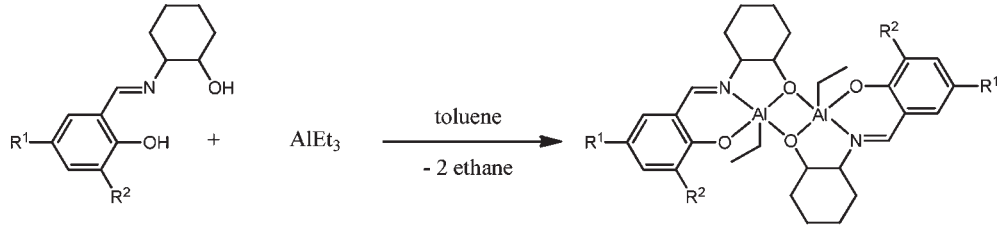

1a : R^1 = *t*-Bu, R^2 = *t*-Bu
1b : R^1 = H, R^2 = OMe
1c : R^1 = Me, R^2 = $SiPh_3$
1d : R^1 = Me, R^2 = $SiMe_2{}^tBu$

2a : R^1 = *t*-Bu, R^2 = *t*-Bu
2b : R^1 = H, R^2 = OMe
2c : R^1 = Me, R^2 = $SiPh_3$
2d : R^1 = Me, R^2 = $SiMe_2{}^tBu$

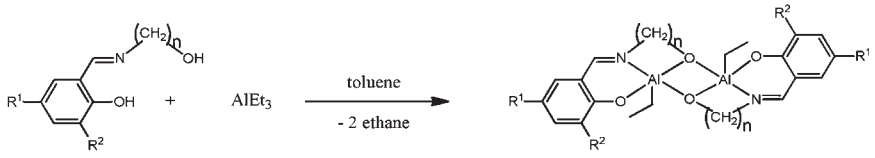

1e : n = 2, R^1 = *t*-Bu, R^2 = *t*-Bu
1f : n = 3, R^1 = *t*-Bu, R^2 = *t*-Bu
1g : n = 4, R^1 = *t*-Bu, R^2 = *t*-Bu
1h : n = 5, R^1 = *t*-Bu, R^2 = *t*-Bu
1i : n = 4, R^1 = Me, R^2 = $SiMe_2{}^tBu$

2e : n = 2, R^1 = *t*-Bu, R^2 = *t*-Bu
2f : n = 3, R^1 = *t*-Bu, R^2 = *t*-Bu
2g : n = 4, R^1 = *t*-Bu, R^2 = *t*-Bu
2h : n = 5, R^1 = *t*-Bu, R^2 = *t*-Bu
2i : n = 4, R^1 = Me, R^2 = $SiMe_2{}^tBu$

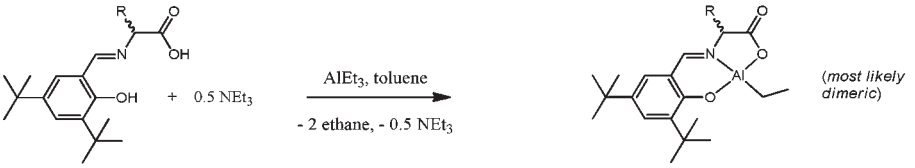

1j : R = 2-(methylthio)ethyl
1k : R = benzyl

2j : R = 2-(methylthio)ethyl
2k : R = benzyl

Scheme 2

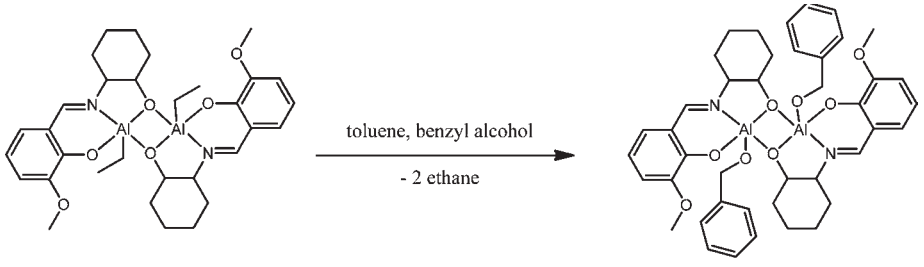

2b **3b**

acids (**2j**,**k**). Suitable single crystals of the chiral amino alcohol complexes **2a** and **2d** were obtained upon recrystallization from dichloromethane at −10 °C. On the other hand, the other two derivatives, **2b** and **2c**, failed to provide single crystals under similar conditions. Instead the addition of 1 equiv of benzyl alcohol to a crystal tube containing complex **2b** afforded crystals of complex **3b**, where the ethyl group was replaced by the benzyloxide group as evidenced by X-ray crystallography (Scheme 2).

The X-ray structures of the closely related aluminum complexes **2a**, **2d**, and **3b** derived from chiral amino alcohols are illustrated in Figure 1, where all complexes are shown to be dimeric. The aluminum centers coordinated to these Schiff base ligands are held together by bridging oxygen atoms with each metal adopting a distorted-bipyramidal geometry with an ethyl group (**2a** and **2d**) or a benzyloxide (**3b**) on the metal centers arranged cis to one another. Selected bond distances and bond angles for these derivatives are provided in Table 1. All bond lengths within the three complexes are quite similar with the exception of the Al(1)−O(1) distance which is slightly shorter in complex **3b** as a result of the electron donating methoxy substituent on the phenoxide ring. The bond angles in complex **3b** were also found to be slightly different from those in complexes **2a** and **2d** because of less steric hindrance of OMe as compared to the bulky ^tBu and $SiMe_2{}^tBu$ substituents on the phenoxide ring.

dx.doi.org/10.1021/ic2008057 |*Inorg. Chem.* 2011, 50, 6775–6787

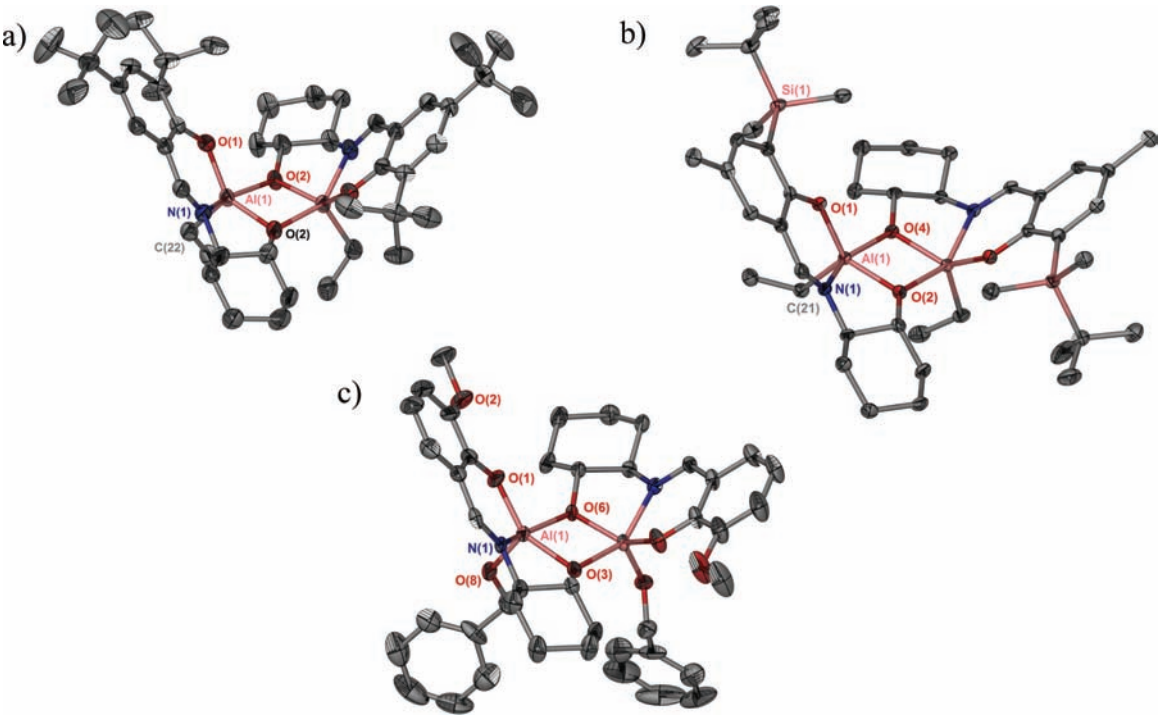

Figure 1. X-ray crystal structures of (a) complex **2a**, (b) complex **2d**, and (c) complex **3b**. Thermal ellipsoids represent the 50% probability levels with hydrogen atoms omitted for clarity.

Table 1. Selected Bond Lengths (Å) and Angles (deg) for Aluminum Complexes 2a, 3b, 2d, 2f (*cis*-), 2f (*trans*-), and 2g (*trans*-)

	2a	3b	2d	2f (*cis*-)	2f (*trans*-)	2g (*trans*-)
			Bond Lengths			
Al(1)−O1	1.811 (2)	1.778 (3)	1.8142 (15)	1.796 (3)	1.797 (4)	1.792 (4)
Al(1)−N1	2.011 (3)	1.978 (4)	2.2041 (18)	2.030 (4)	2.034 (4)	2.047 (5)
Al(1)−X[a]	1.873 (2)	1.850 (3)	1.8716 (15)	1.846 (3)	1.851 (3)	1.831 (5)
Al(1)−Y[b]	1.899 (2)	1.899 (3)	1.8959 (15)	1.915 (3)	1.905 (3)	1.935 (5)
Al(1)−Z[c]	1.963 (3)	1.733 (3)	1.977 (2)	1.992 (5)	1.993 (5)	2.002 (7)
			Bond Angles			
O(1)−Al(1)−N(1)	88.31 (10)	90.26 (16)	88.93 (7)	88.75 (14)	89.83 (16)	90.3 (2)
O(1)−Al(1)−X[a]	94.78 (10)	92.39 (15)	97.19 (7)	89.61 (13)	92.14 (16)	91.3 (2)
[a]X−Al(1)−Y[b]	75.30 (10)	76.66 (14)	74.61(6)	75.94 (14)	74.91 (17)	77.2 (2)
[b]Y−Al(1)−N(1)	79.52 (10)	82.12 (15)	79.36 (7)	88.58 (14)	87.52 (16)	90.6 (2)
O(1)−Al(1)−Z[c]	111.65 (13)	108.04 (18)	110.56 (8)	113.62 (17)	113.4 (2)	116.2 (3)
N(1)−Al(1)−X[a]	147.29 (11)	145.38 (16)	149.03 (7)	157.52 (15)	158.63 (17)	167.1(2)

[a] X = O(2) (red), O(6), O(2), O(2) (red), O(2) (red), O(2) (red) in **2a**, **3b**, **2d**, **2f** (*cis*-), **2f** (*trans*-), **2g**, respectively. [b] Y = O(2) (black), O(3), O(4), O(2) (black), O(2) (black), O(2) (black) in **2a**, **3b**, **2d**, **2f** (*cis*-), respectively. [c] Z = C(22), O(8), C(21), C(19), in **2a**, **3b**, **2d**, **2f** (*cis*-) respectively.

The solid state structures of the aliphatic amino alcohol derivatives of aluminum were also obtained in this study. As we previously noted based on variable-temperature ^{1}H NMR studies, in these instances the isomer isolated, that is, *cis* or *trans* arrangement of apical ligands, depends on temperature.[12] For example, complex **2g** was recrystallized following heating of the complex at 50 °C in methylene chloride in a sealed tube until complete dissolution. Upon cooling the solution and maintaining it at −10 °C, the trans isomer was exclusively afforded (Figure 2a). On the other hand, complex **2f** was dissolved in methylene chloride at ambient temperature and kept at −10 °C resulting in formation of crystals of both cis and trans isomers. The two five-coordinate aluminum centers in this series of aluminum complex possess distorted-bipyramidal geometries with the ethyl groups on each metal center *cis* to one another in complex **2f** (*cis*) and *trans* to each other in complex **2f** (*trans*) and **2g**. Thermal ellipsoid representations of these structures are shown in Figure 2, with selected bond distances and bond angles listed in Table 1. Although we have thus far not been successful in obtaining crystals of complexes **2j** and **2k**, these are most likely similarly dimeric in structure.

POLYMERIZATION STUDIES

Ring-Opening Polymerization of Lactides. The aluminum complexes shown in Scheme 1 were examined as catalysts for the

dx.doi.org/10.1021/ic2008057 |*Inorg. Chem.* 2011, 50, 6775–6787

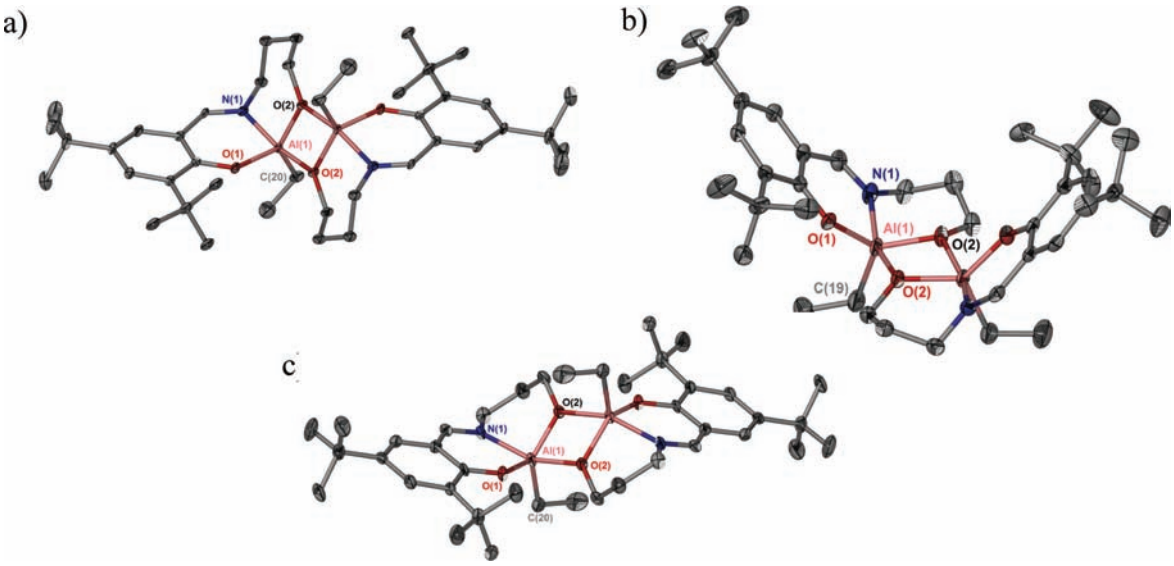

Figure 2. X-ray crystal structures of (a) **2g** (*trans*-), (b) **2f** (*cis*), and (c) **2f** (*trans*-). Thermal ellipsoids represent the 50% probability surfaces. Hydrogen atoms are omitted for the sake of clarity.

Table 2. Reactivity and Selectivity of Aluminum Complexes 2a−k for the ROP of *rac*-lactide[a]

					M_n			
entry	M	time (h)	conversion (%)[b]	*meso*-[c]	theoretical[d]	$0.58M_{n,}$ GPC[e]	PDI	P_m(%)[f]
1	**2a**[g]	20	0	no				
2	**2a**[h]	66	0	yes				
3	**2a**	15	0	yes				
4	**2a**	66	57	yes	4 107	7 938	1.05	70
5	**2b**	15	0	yes				
6	**2b**	69	43	yes	3 243	3 844	1.08	<50
7	**2c**	15	0	yes				
8	**2c**	168	45	yes	3 207	4 962	1.09	<50
9	**2d**	15	0	yes				
10	**2e**	15	64	yes	4 614	6 987	1.04	62
11	**2f**	15	0	yes				
12	**2g**	15	34	no	2 446	2 456	1.07	76
13	**2h**	15	50	no				73
14	**2i**	15	21	no				82
15	**2j**	15	36	no	2 594	3 916	1.07	74
16	**2k**	15	42	no	3 026	4 043	1.03	72

[a] Unless otherwise specified, the polymerization reactions were performed in sealed reaction tubes with the following conditions: [*rac*-LA]/[Al] = 50, in toluene at 70 °C. [b] Obtained from ^{1}H NMR spectroscopy. [c] *meso*-lactide was obtained from epimerization of L- or D-lactide during the polymerization process. [d] Theoretical M_n = (M/I) x (% conversion) x (mol. wt. of lactide). [e] M_n values were corrected by the equation: $M_n = 0.58\ M_{n,\ GPC}$.[13] [f] P_m values were calculated from the ratio of the (area of iii)/(total area in methine proton region). [g] $CDCl_3$ was used as the solvent at ambient temperature. [h] $CDCl_3$ was used as the solvent at 60 °C.

ROP of *rac*-lactide in solution, where Table 2 summarizes the relative reactivity and selectivity observed for this polymerization process under similar reaction conditions. Although complex **2a** was not efficient at catalyzing *rac*-lactide in $CDCl_3$ after an extended period of time at 60 °C (*entry 2*); over the same time period a 57% conversion to polylactide was noted in toluene at 70 °C (*entry 4*). In the series of aluminum complexes **2a**−**d** when the substituents (R^2) on the phenoxide portion of the Schiff base ligand increased in size (R^2 = $SiPh_3$) or is more electron donating (R^2 = OMe), the rate of polymerization decreased (*entries 6 and 8*). Similar results have been reported previously in related systems by Gibson and co-workers,[14a] as well as by Nomura and co-workers.[14b] Complex **2a** afforded a moderately isotactic polylactide with a P_m value of 0.70, whereas, complexes **2b**, **c** produced atactic polylactide with P_m values less than 0.50. The aluminum complexes with achiral aliphatic backbones with the exception of **2f**, that is, complexes **2e**, **g**, **h**, **i**, were observed to polymerize *rac*-lactide at faster rates than complex **2a** to provide isotactic polymers with P_m values of 0.62, 0.76, 0.73, and 0.82, respectively. It should also be noted here that when the substituents on the phenoxide (R^2) of the half-salen ligand in the series of complexes **2e**−**i** increased in size from ^{t}Bu to $SiMe_2{}^t$Bu, the percent of isotacticity of the polymer increased from 0.76 to 0.82.

The complexes derived from *rac*-amino acids, **2j** and **2k**, were also active for catalyzing the ROP of *rac*-lactide, providing isotactic polylactide with P_m values of 0.74 and 0.72 as shown in Table 2. Previously we established that aluminum complexes which existed in both *cis* and *trans* forms, e.g., **2e** and **2f**, under conditions of the ring-opening polymerization reaction led to partial epimerization of D- and L-lactide to *meso*-lactide prior to polymerization.[12] Similarly, upon utilizing complexes **2a**−**d** as catalysts for the ROP of *rac*-lactide, *meso*-lactide was observed to be produced during the polymerization process. Presumably, the *cis* isomeric form of the series of complexes **2a**−**d** is responsible for the formation of *meso*-lactide. As evident from X-ray crystallography only the *cis* isomeric form of complexes **2a**, **3b**, and **2d** was obtained in the solid state. On the contrary, when complexes which exist in the *trans* isomeric form are used to catalyze the ROP of *rac*-lactide in toluene at 70 °C, no epimerization was observed and concomitantly a polylactide was produced with a high degree of isotacticity (P_m = 82%).

There are two proposed mechanisms for the stereoselective ROP of *rac*-lactide,[15] that is, an enantiomorphic site-control,[16] and a chain-end control mechanism.[14b] Chisholm and co-workers have shown in addition to chiral ligands bound to aluminum

dx.doi.org/10.1021/ic2008057 |*Inorg. Chem.* 2011, 50, 6775–6787

Scheme 3

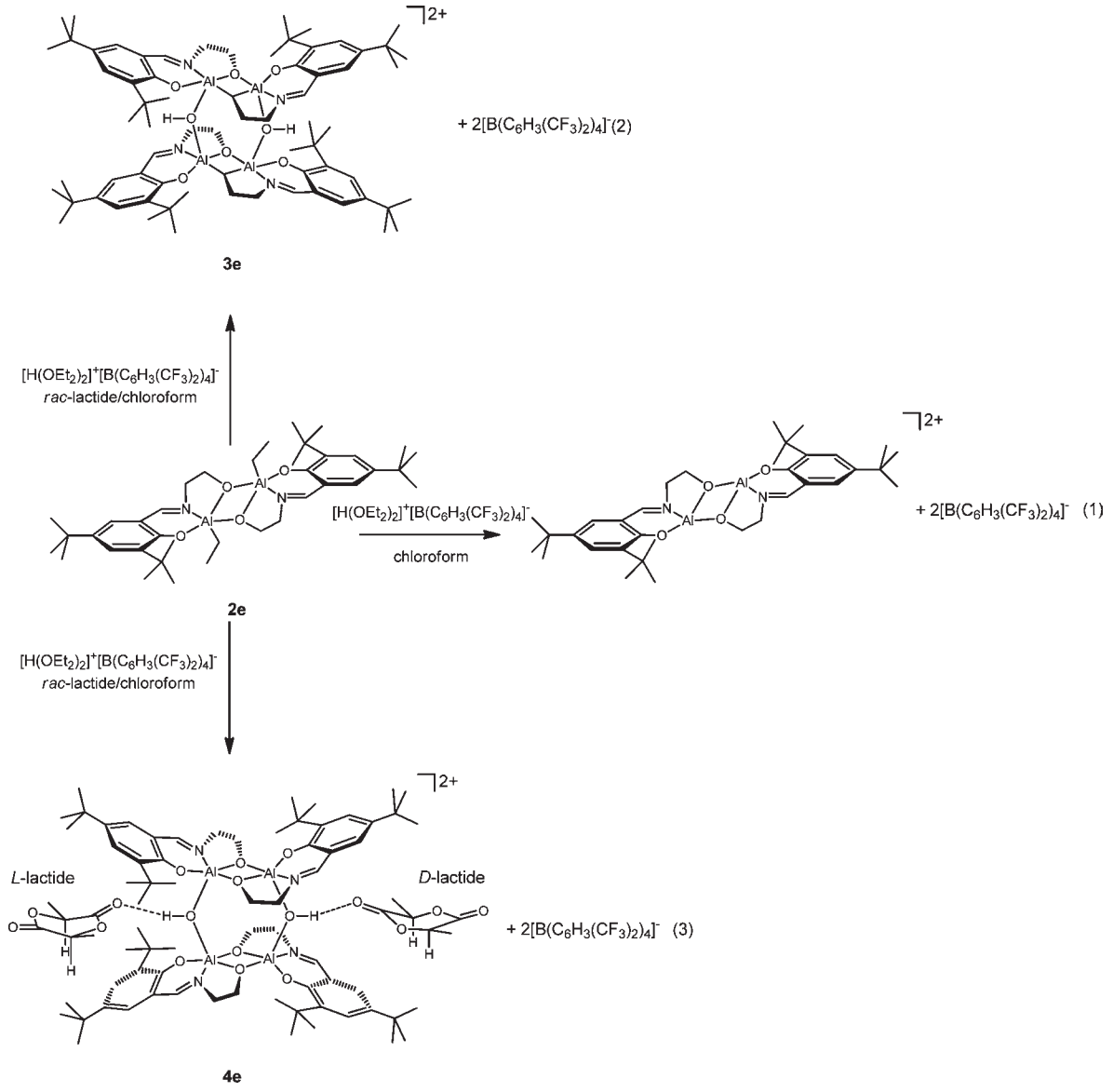

centers, other factors can also contribute to the stereoselectivity in the ROP of lactides when utilizing aluminum salen complexes as catalysts.[17] These include considerations of the chirality of the initiator as well as the solvent. To better understand the origin of the stereoselectivity of *rac*-lactide during the polymerization process in our catalytic system, we attempted to obtain crystal structures of lactide binding to the aluminum centers in our complexes. The ethyl group on the aluminum center can be removed upon reaction with $[H(OEt_2)_2]^+$ $[B(C_6H_3(CF_3)_2)_4]^-$ as illustrated in eq (1) in Scheme 3. Zwitterion formation and aryl transfer to aluminum can be avoided when using the non-nucleophilic $[B(C_6H_3(CF_3)_2)_4]^-$ as counteranion.[18] X-ray quality crystals obtained from a $CHCl_3$ solution of complex **2e** in the presence of $[H(OEt_2)_2]^+$ $[B(C_6H_3(CF_3)_2)_4]^-$ and 1 equiv of *rac*-lactide were found to consist of two morphological forms, that is, plate-like and block-like crystals. The plate-like crystals were shown to be a tetrameric aluminum complex with two $[B(C_6H_3(CF_3)_2)_4]^-$ counterions. All four aluminum centers are five-coordinate with bridging oxygen atoms from the Schiff base ligands and hydroxyl groups as illustrated in Figure 3 and Scheme 3, eq 2. The molecular structure of the block-like crystals are also tetrameric and similar to that observed in **3e**, except the ^{t}Bu substituents were found in this derivative, complex **4e**, on opposite sides as seen in Figure 4 and Scheme 3, eq 3. In addition, complex **4e** contains two lactide molecules located between the phenoxides of the half-salen ligands with hydrogen bonds from the carbonyl oxygen of the lactide to the bridging hydroxyl ligands (1.876 Å). Both L-lactide (left) and D-lactide (right) were found in the solid state structure as shown in Figure 4 and Scheme 3, eq 3. This observation suggests that the stereoselectivity noted for the ROP of *rac*-lactide in the presence of the aluminum complexes **2e**−**i** results from an enantiomorphic site control mechanism dictated by the bulky ^{t}Bu substituents in the R^1 position. The bond distance of Al1−O9 of 1.805 Å lies within

dx.doi.org/10.1021/ic2008057 |*Inorg. Chem.* 2011, 50, 6775–6787

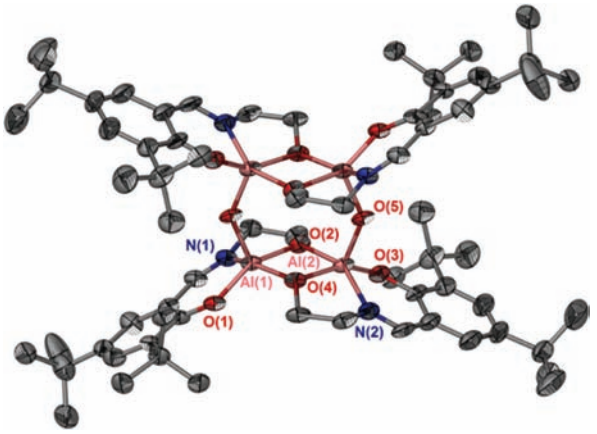

Figure 3. X-ray crystal structure of complex **3e**. Thermal ellipsoids represent the 50% probability surfaces. Hydrogen atoms and $2[B(C_6H_3-(CF_3)_2)_4]^-$ are omitted for the sake of clarity. Selected bond lengths (Å) and angles (deg): Al1−N1: 1.944 (4), Al1−O1: 1.779 (4), Al1−O2: 1.873 (4), Al1−O4: 1.862 (3), Al2−N2: 1.959 (4), Al2−O3: 1.765 (4), Al2−O4: 1.876 (4), Al2−O5: 1.817 (4), N1−Al1−O1: 92.06 (18), N1−Al1−O2: 82.50 (17), O1−Al1−O4: 96.97 (16), O2−Al1−O4: 76.15 (15), N1−Al1−O4: 150.00 (19), O1−Al1−O2: 152.03 (17), N2−Al2−O3: 91.67 (19), N2−Al2−O4: 81.80 (17), O2−Al2−O4: 76.79 (15), O2−Al2−O3: 97.18 (17), N2−Al2−O2: 150.29 (19), O3−Al2−O4: 151.12 (18), O3−Al2−O5: 105.53 (18).

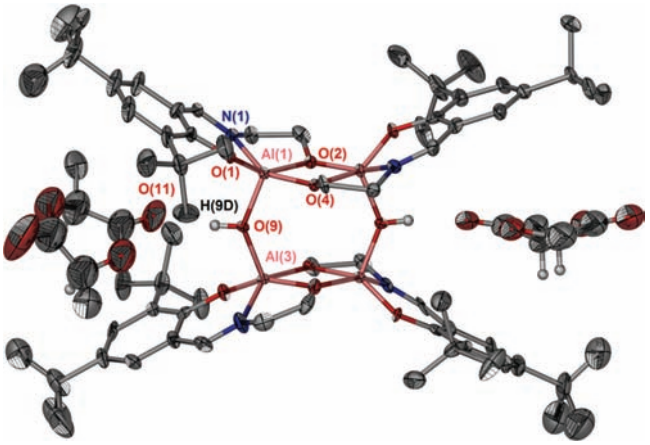

Figure 4. X-ray crystal structure of complex **4e**. Thermal ellipsoids represent the 50% probability surfaces. Hydrogen atoms and $2[B(C_6H_3-(CF_3)_2)_4]^-$ are omitted for the sake of clarity. Selected bond lengths (Å) and angles (deg): Al1−N1: 1.948 (8), Al1−O1: 1.756 (7), Al1−O2: 1.886 (6), Al1−O4: 1.839 (6), Al1−O9: 1.805 (6), O11−H9D: 1.876 (8), N1−Al1−O1: 92.4 (3), N1−Al1−O2: 81.7 (3), O2−Al1−O4: 76.5 (3), O1−Al1−O4: 96.7 (3), N1−Al1−O4: 149.7 (3), O1−Al1−O2: 151.4 (3), O1−Al1−O9: 104.6 (3), Al1−O9−Al3: 139.2 (3).

the range of those reported in the literature.[19] We assume the hydroxyl bridging ligands result from adventitious water being present during the crystal growth process.

Ring-Opening of Other Cyclic Monomers. Complex **2g** was selected to investigate the ring-opening polymerization for other cyclic monomers (Chart 1) because of its greater reactivity and selectivity compared to the other aluminum complexes for the ROP of lactides. Table 3 summarizes the reactivity of complex **2g** for the various cyclic monomers in toluene at 70 °C with a monomer/initiator ratio (M/I) of 50:1. The percent conversion

Chart 1

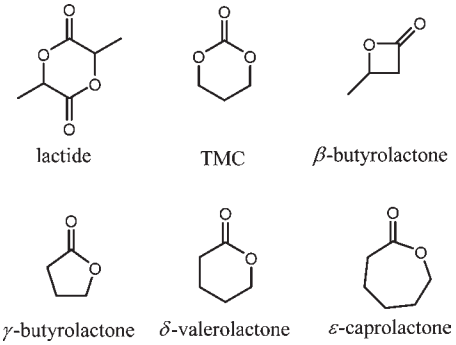

Table 3. Reactivity of Aluminum Complex 2g for the ROP of Cyclic Monomers[a]

			M_n		
entry	monomer	conversion (%)[b]	theoretical[c]	$M_{n,GPC}$	PDI
1	*rac*-lactide	34	2 446	2 456[d]	1.07
2	TMC	99	5 050	2 567	1.66
3	*rac*-β-butyrolactone	26	1 118	1 450	1.23
4	γ-butyrolactone[e]	0	N/A	N/A	N/A
5	δ-valerolactone	30	1 501	1 819	1.89
6	ε-caprolactone	99	5 649	2 356	1.75

[a] Unless otherwise specified, the polymerization reactions were performed in sealed reaction tubes with the following conditions: monomer/[Al] = 50, in toluene at 70 °C. [b] Obtained from ^{1}H NMR spectroscopy. [c] Theoretical M_n = (M/I) × (% conversion) × (mol. wt. of lactide). [d] M_n values were corrected by the equation: $M_n = 0.58\ M_{n,\ GPC}$.[13] [e] The reaction was performed in toluene at 70 and 105 °C.

of each monomer to polymer was monitored by ^{1}H NMR after 15 h of reaction, with the resulting polymers isolated and purified by precipitation from CH_2Cl_2 with 5% HCl in methanol followed by drying in vacuo.

As indicated in Table 3, complex **2g** was found to catalyze all of the cyclic monomers examined except for the five-membered cyclic lactone (γ-butyrolactone), even at 105 °C in toluene. This is explained based on the fact that the geometric distortion in the ester group in γ-butyrolactone is much less than that in δ-valerolactone resulting in lower ring strain.[20] Complex **2g** was more effective at catalyzing the ROP of trimethylene carbonate and ε-caprolactone than the other cyclic monomer, with 99% conversion being observed in 15 h. Although complex **2g** catalyzed the ROP of *rac*-lactide to isotactic polylactide with a P_m value of 0.76, β-butyrolactone similarly underwent ROP to afford an atactic polymer as evidenced by ^{13}C NMR spectroscopy.[21] The dependence of the molecular weights of polylactide and poly-β-butyrolactone produced on the monomer/initiator ratios was investigated and the results are provided in Tables 4 and 5, respectively. As illustrated in Figure 5 there is a linear correlation of M_n and the monomer/initiator ratio, indicative of a well-controlled polymerization process. The living character of these polymerization processes is further noted in the low polydispersities observed, where the PDIs for polylactide and poly-β-butyrolactone span the range of 1.09−1.18 and 1.12−1.18, respectively. However, the molecular weights of

dx.doi.org/10.1021/ic2008057 |*Inorg. Chem.* 2011, 50, 6775–6787

Table 4. Polylactide Produced from the ROP of *rac*-lactide in Toluene at 70 °C

			M_n			
entry	M/I	conversion (%)[a]	theoretical[b]	GPC	$0.58M_{n,GPC}$[c]	PDI
1	115	96	15 913	28 024	16 254	1.12
2	155	96	21 448	40 598	23 457	1.09
3	230	96	31 826	59 694	34 632	1.18
4	460	96	63 552	109 513	63 518	1.10

[a] Obtained from ^{1}H NMR spectroscopy. [b] Theoretical M_n = (M/I) × (% conversion) × (mol. wt. of lactide). [c] M_n values were corrected by the equation: $M_n = 0.58M_{n,\ GPC}$.[13]

Table 5. Poly-*β*-butyrolactone Produced from the ROP of *β*-Butyrolactone in Toluene at 70 °C

				M_n		
entry	M/I × monomer conversion	M/I	conversion (%)[a]	theoretical[b]	GPC	PDI
1	142	160	89	12 347	12 753	1.12
2	177	217	82	15 235	15 601	1.22
3	202	317	64	17 552	18 248	1.28

[a] Obtained from ^{1}H NMR spectroscopy. [b] Theoretical M_n = (M/I) × (% conversion) × (mol. wt. of *β*-butyrolactone).

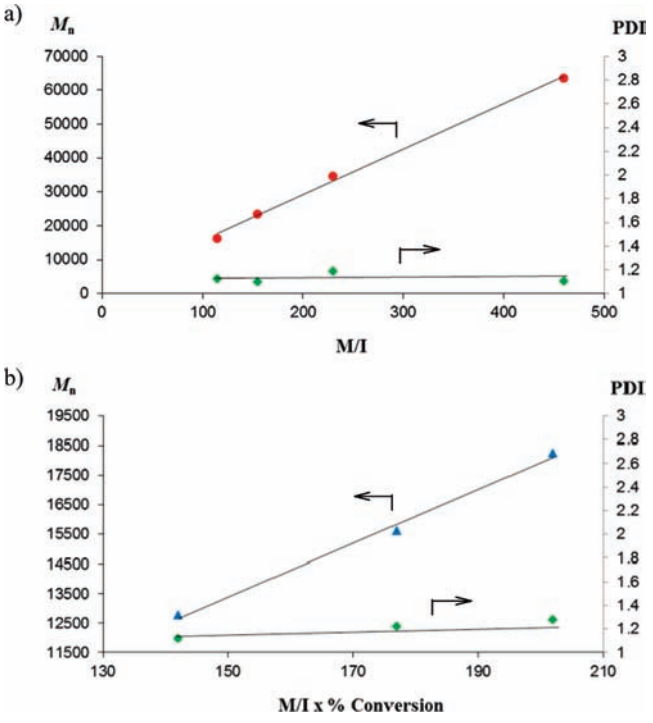

Figure 5. (a) Linear relationship observed between M_n and monomer/initiator ratio of polylactide from *rac*-lactide catalyzed by complex **2g** at 70 °C in toluene. (b) Linear relationship observed between M_n and monomer/initiator ratio of poly-*β*-butyrolactone from *rac*-*β*-butyrolactone catalyzed by complex **2g** at 70 °C in toluene.

poly(TMC), poly-*δ*-valerolactone, and poly-*ε*-caprolactone observed for the polymers produced by the ROP of the corresponding

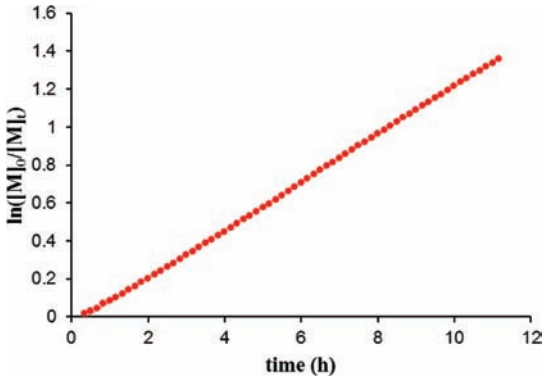

Figure 6. Plot of ln([*rac*-LA]$_0$/[*rac*-LA]$_t$) vs time depicting a reaction order of unity with respect to monomer concentration (R^2 = 0.999).

monomers catalyzed by complex **2g** did not agree with the expected values. Furthermore, the PDIs of these polymers were found to be rather broad, see Table 3. These results are suggestive of transesterification occurring during the polymerization process possibly resulting from less steric hindrance of the alkoxide formed at the metal center from the ring-opening of these cyclic monomers.

Kinetic Studies of the Ring-Opening Polymerization of *rac*-lactide. Kinetic measurements of the ring-opening polymerization of *rac*-lactide were carried out in modest pressure NMR tubes employing complex **2g** as catalyst in toluene solution. *It should be noted here that rac-lactide is not very soluble in deuterated toluene at ambient temperature; therefore, all reactions were preheated at 90 °C prior to being placed in the preheated NMR spectrometer.* The observed rate constants (k_{obsd}) were extracted from a plot of ln([*rac*-LA]$_0$/[*rac*-LA]) versus time (Figure 6). The reaction order in catalyst concentration was determined from a plot of k_{obsd} versus [Al] and the ln[k_{obsd}] versus ln[Al] as shown in Figure 7. As seen from the linearity of the plot of k_{obsd} versus [catalyst] as well as the near unity of the slope of the ln[k_{obsd}] versus ln[catalyst] plot, the ROP of *rac*-lactide in the presence of complex **2g** is first order in catalyst concentration. This kinetic data is listed in Table 6, along with analogous temperature dependent data. The activation parameters for the ROP of *rac*-lactide catalyzed by complex **2g** in deuterated toluene were determined from the data in Table 6 to be $\Delta H^{\ddagger}$ = 59.7 ± 2.8 kJ/mol and $\Delta S^{\ddagger}$ = −129.1 ± 7.7 J/mol K (see Eyring plot in Figure 8). The corresponding free energy of activation for this polymerization process was calculated to be 106.6 kJ/mol at 90 °C.

Kinetic measurements of the ring-opening polymerization of the other cyclic monomers examined in this report were conducted in the same manner as those for *rac*-lactide. The polymerization processes were shown to be first-order in monomer concentration for all monomers investigated as evidenced by the plot of ln([M]$_0$/[M]$_t$) versus time as depicted in Figure 9. Table 7 listed the k_{obsd} values for each monomer as a function of both catalyst concentration and temperature. It is noteworthy that in each case there is a brief initiation period involved. Furthermore, plots of ln[k_{obsd}] versus ln[Al] as shown in Figure 10 reveal the order of the reaction with respect to catalyst (**2g**) concentration to be 0.73, 0.85, 0.48, and 0.55 for the ROP of TMC, *rac*-*β*-BL, *δ*-VL, and *ε*-CL, respectively. Fractional dependencies on [catalyst] have previously been reported for the ROP of lactones with other aluminum complexes.[22] A fractional order on [catalyst] can be explained by an aggregation of the active species during the polymerization process. Hence, a determination of the propagation rate constant (k_p) in

dx.doi.org/10.1021/ic2008057 |*Inorg. Chem.* 2011, 50, 6775–6787

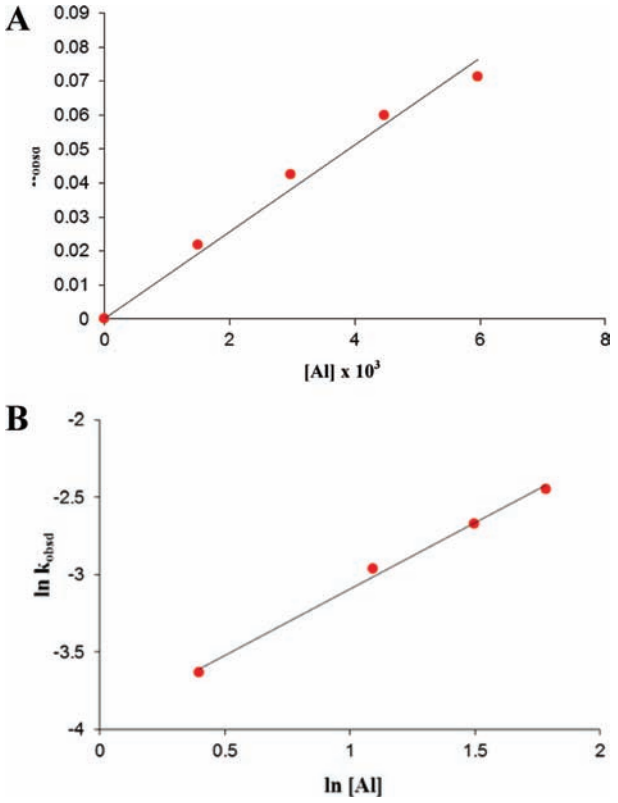

Figure 7. (**A**) Plot of k_{obsd} vs [Al] with slope = 0.0128 and R^2 = 0.9822. (**B**) Plot of ln k_{obsd} vs ln[Al] with slope = 0.86 and R^2 = 0.984.

Table 6. Rate Constants Dependence on the Concentration of the Catalyst (2g) and Temperature for the Ring-Opening Polymerization of *rac*-Lactide[a]

entry	[Al] (mM)	temp (°C)	k_{obsd} (h^{-1})	k_p (M^{-1}-sec^{-1})
1	1.49	90	0.0219	3.77×10^{-3} [b]
2	2.98	90	0.0424	3.77×10^{-3} [b]
3	4.47	90	0.0600	3.77×10^{-3} [b]
4	5.96	90	0.0713	3.77×10^{-3} [b]
5	4.47	80	0.0304	1.89×10^{-3}
6	4.47	100	0.0985	6.12×10^{-3}
7	4.47	105	0.126	7.85×10^{-3}

[a] Monomer concentration was held constant at 0.69 M and reactions carried out in toluene-d_8. [b] Average value for entries 1−4.

the polymerization process is complicated.[23] The fractional order will be equal to the reciprocal of the degree of aggregation when the majority of the active species is aggregated and only a small fraction is unaggregated.[24]

It is apparent that the steric of methyl group on polylactide and poly-β-BL affects the degree of aggregation during the polymerization process. The more steric alkoxide resulting from the ROP of a *rac*-lactide and *rac*-β-BL monomer is a secondary alkoxide. The more steric hindrance of this methyl group should decrease the degree of aggregation during the polymerization process when compared to the primary alkoxide derived from the ROP of TMC, δ-VL, and ε-CL. The rates for the ROP of each cyclic monomer under the same condition were compared (entry 4, Table 7). The experimental results indicated that complex **2g** catalyzed ε-CL and TMC at similar rates with k_{obsd} values of

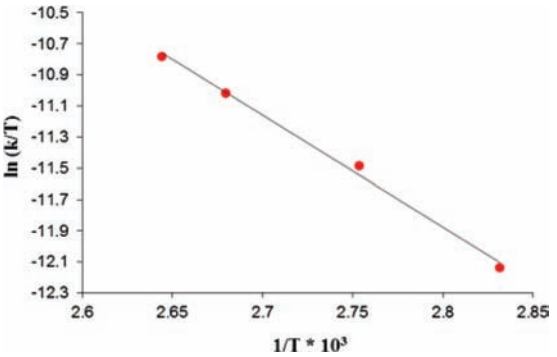

Figure 8. Eyring plot of ROP of *rac*-lactide in the presence of catalyst **2g** in toluene-d_8. Slope = −7180 with R^2 = 0.995.

2.25 h^{-1} and 2.16 h^{-1}, respectively. The k_{obsd} value for the ROP of δ-VL (0.119 h^{-1}) catalyzed by complex **2g** is slightly higher than that of the polymerization reactions of *rac*-β-BL (0.0692 h^{-1}) and *rac*-lactide (0.0600 h^{-1}).

The ring-opening polymerizations of *rac*-β-BL, TMC, δ-VL, and ε-CL were carried out over the temperature range 70−105 °C to obtain the activation parameters for these processes. The activation parameters $\Delta H^{\ddagger}$ and $\Delta S^{\ddagger}$ calculated from the Eyring plot shown in Figure 11 were determined and are listed in Table 8. The $\Delta G^{\ddagger}$ values for the ROP of these cyclic monomers at 90 °C were also calculated and listed in Table 8. The $\Delta G^{\ddagger}$ values at 90 °C of 95.4 and 95.2 kJ/mol for the ROP of TMC and ε-CL are similar. This results demonstrates that the two processes are energetically the same. Likewise, the $\Delta G^{\ddagger}$ values at 90 °C for the ROP of *rac*-lactide (106.6 kJ/mol) and *rac*-β-BL (106.3 kJ/mol) were similar and are slightly higher than the $\Delta G^{\ddagger}$ value for the ROP of δ-VL (104.5 kJ/mol) at 90 °C.

Copolymerization of Cyclic Monomers. Although complex **2g** was shown to effectively catalyze the ROP of *rac*-lactide and *rac*-β-BL in toluene at 90 °C with similar k_{obsd} values (0.060 h^{-1} versus 0.069 h^{-1}, see Table 7), in a copolymerization reaction (50:50 monomer feed) only *rac*-lactide was polymerized after an extended time period with no evidence of polybutyrolactone being formed. A similar copolymerization reaction was carried out involving *rac*-lactide and δ-VL. In this instance a tapered polylactide-polyvalerolactone copolymer, where the lactide monomer conversion was initially high, was obtained as evidenced by ^{1}H NMR spectroscopy. A series of experiments were performed as indicated in Table 9 to determine the monomer reactivity ratios as defined by the Fineman−Ross eqs 4 and 5.[25] From the mole fraction of δ-VL in the monomer feed (F) and in the copolymer (f) as determined by ^{1}H NMR spectroscopy of the purified copolymer, a Fineman−Ross plot was created as indicated in Figure 12.

$$\frac{(f-1)}{F} = -r_{lactide}\frac{f}{F^2} + r_{valero} \qquad (4)$$

$$r_{lactide} = \frac{k_{LL}}{k_{LV}} \quad \text{and} \quad r_{valero} = \frac{k_{VV}}{k_{VL}} \qquad (5)$$

The reactivity ratios determined from the slope ($r_{lactide}$) and the intercept (r_{valero}) of the Fineman−Ross plot were found to be 2.78 and 0.140, respectively. The value of $r_{lactide}$ indicates that the polymer's lactide unit prefers to ring open *rac*-lactide over δ-VL, and the r_{valero} designates that upon insertion of δ-VL in the polymer chain, it also prefers to ring open a *rac*-lactide monomer

dx.doi.org/10.1021/ic2008057 |*Inorg. Chem.* 2011, 50, 6775–6787

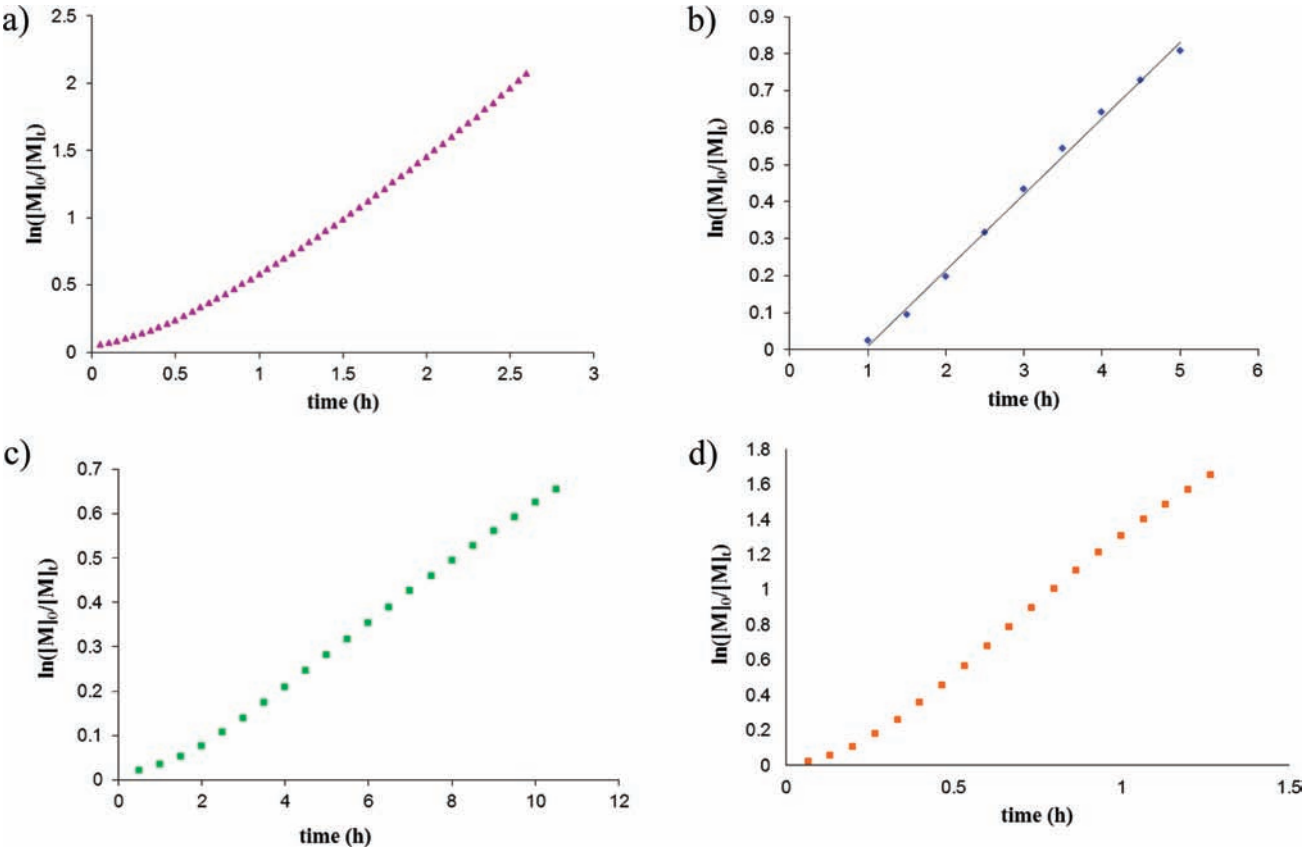

Figure 9. Plot of $\ln([M]_0/[M]_t)$ vs time depicting a reaction order of unity with respect to (a) [TMC] (R^2 = 0.987), (b) [*rac*-β-BL] (R^2 = 0.996), (c) [δ-VL] (R^2 = 0.997), and (d) [ε-CL] (R^2 = 0.995).

Table 7. Rate Constants Dependence on the Concentration of the Catalyst (2g) and Temperature in the ROP of Cyclic Monomers[a]

entry	[Al] (mM)	temp (°C)	*rac*-lactide k_{obsd} (h^{-1})	TMC k_{obsd} (h^{-1})	*rac*-β-BL k_{obsd} (h^{-1})	δ-VL k_{obsd} (h^{-1})	ε-CL k_{obsd} (h^{-1})
1	0.74	90				0.047	
2	1.49	90	0.0219	1.00	0.0264		1.28
3	2.98	90	0.0424	1.66	0.0519	0.0777	1.82
4	4.47	90	0.0600	2.16	0.0692	0.119	2.25
5	5.96	90	0.0713	2.80	0.0868	0.128	2.78
6	4.47	70		0.886		0.0355	
7	4.47	80	0.0304	1.54	0.0230	0.0617	1.46
8	4.47	100	0.0985		0.148	0.174	4.03
9	4.47	105	0.126	4.09	0.205		5.37

[a] Monomer concentration was held constant at 0.69 M and reactions carried out in toluene-d_8.

as opposed to a δ-VL monomer. This result clearly demonstrates that a tapered polylactide-polyvalerolactone copolymer with high lactide composition should be observed early on in the copolymerization process. A purified copolymer, which was precipitated from 5% HCl in methanol followed by drying, with a composition of *rac*-lactide to δ-valerolactone of 6.50:1.74 (entry 3 in Table 9) displayed a M_n value of 9600 (PDI = 1.69). The T_g of this copolymer was determined to be 7.69 °C which lies between the T_g of pure polylactide (55 °C) and poly-δ-VL (−63 °C).[26]

Kinetic measurements of the copolymerization of *rac*-lactide and δ-VL catalyzed by complex **2g** in deuterated toluene were carried out at 90 °C and monitored by ^{1}H NMR spectroscopy. As expected based on the Fineman−Ross analysis above the rate of enchainment of *rac*-lactide was observed to be faster than that of δ-VL. The copolymerization process was found to be first order in both *rac*-lactide and δ-VL concentrations as illustrated from the plots of $\ln([M]_0/[M]_t)$ versus time in Figure 13. As previously noted in the homopolymerization processes there is a brief initiation period seen in the copolymerization process. From the plots of k_{obsd} versus [catalyst] or ln k_{obsd} versus ln[catalyst], the reaction order in complex **2g** concentration was also found to be unity (Figure 14). Table 10 lists the rate constants (k_{obsd}) for the copolymerization of *rac*-lactide and δ-VL as a function of both catalyst concentration and temperature. Hence, the rate

dx.doi.org/10.1021/ic2008057 |*Inorg. Chem.* 2011, 50, 6775–6787

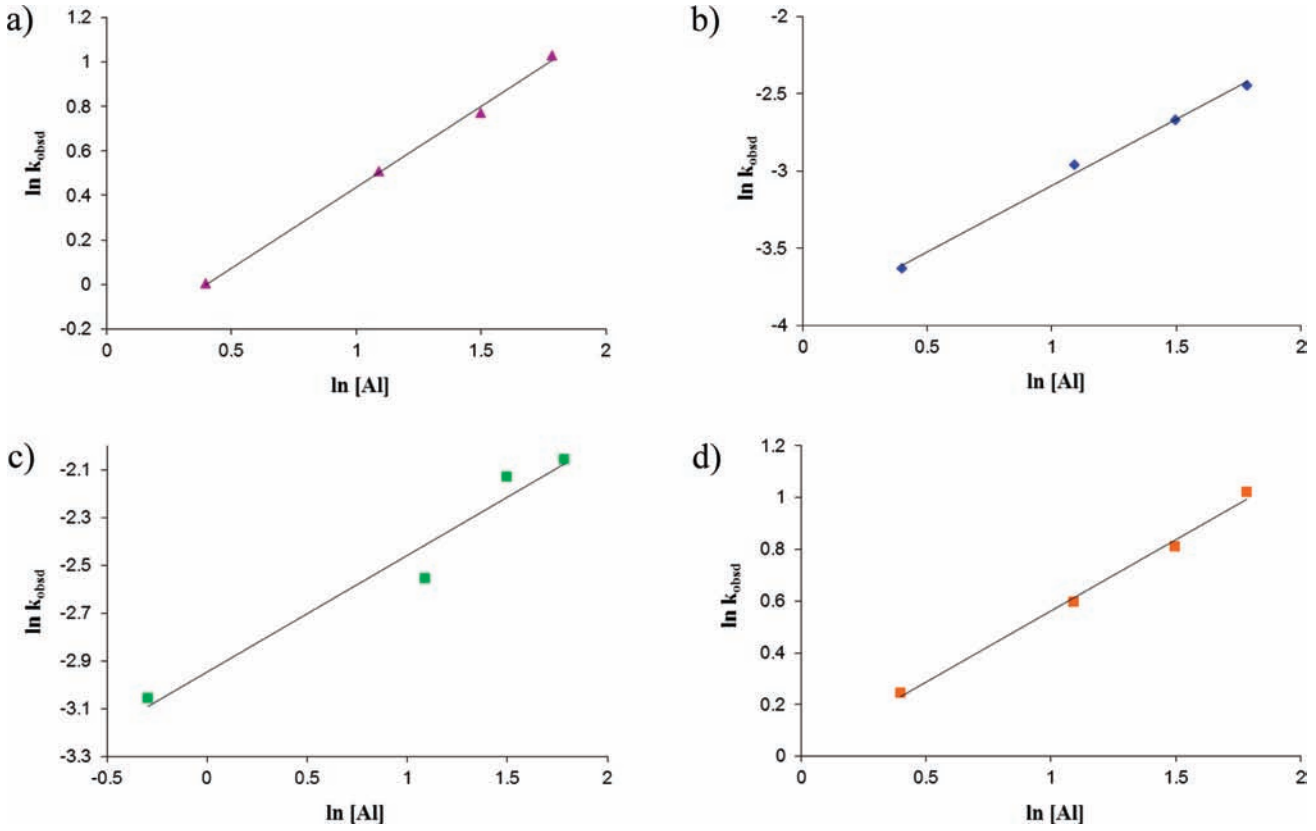

Figure 10. Plot of ln k_{obsd} vs ln[Al] from the ROP of (a) TMC (slope = 0.73, R^2 = 0.997), (b) *rac*-β-BL (slope = 0.85, R^2 = 0.994), (c) δ-VL (slope = 0.48, R^2 = 0.954), and (d) ε-CL (slope = 0.54, R^2 = 0.994).

law for the copolymerization process can be expressed as shown in eq 6.

$$\text{rate} = (k_{LA}[\textit{rac}\text{-lactide}] + k_{\delta\text{-VL}}[\delta\text{-VL}])[\text{Al}] \qquad (6)$$

The activation parameters for the enchainment of *rac*-lactide and δ-VL in the copolymerization reaction were calculated from the temperature dependent data in Table 10. In both instances the $\Delta H^{\ddagger}$ values for the copolymerization processes were larger and the $\Delta S^{\ddagger}$ values less negative than for the corresponding homopolymerization processes. Table 11 compiles the Eyring derived activation parameter for the two ROP processes, which illustrates the observation that the $\Delta G^{\ddagger}$ at 90 °C for the copolymerization and homopolymerization processes are quite similar. Nevertheless, the $\Delta G^{\ddagger}$ for the ROP of δ-VL in the copolymerization has increased somewhat as anticipated from the Fineman–Ross analysis.

SUMMARY

In conclusion, a series of aluminum complexes have been prepared from triethylaluminum and tridentate Schiff base ligands derived from chiral or achiral amino alcohols or amino acids, and have been characterized in both solution and the solid state. These new aluminum complexes were demonstrated to be active in the ring-opening polymerization of *rac*-lactide with reasonably good control over the polymerization process. For example, isotactic polylactide with a P_m as high as 0.82 was obtained. In addition, the most active of these aluminum complexes was shown to catalyze the ring-opening polymerization of trimethylene carbonate, *rac*-β-butyrolactone, δ-valerolactone, and ε-caprolactone. The free energies of activation for these polymerization processes were determined at 90 °C and found to be as follows: $\Delta G^{\ddagger}_{LA}$ (106.6 kJ/mol) ≈ $\Delta G^{\ddagger}_{BL}$ (106.3 kJ/mol) > $\Delta G^{\ddagger}_{VL}$ (104.5 kJ/mol) > $\Delta G^{\ddagger}_{TMC}$ (95.4 kJ/mol) ≈ $\Delta G^{\ddagger}_{CL}$ (95.2 kJ/mol). On the other hand, the free energies of activation for the copolymerization of *rac*-lactide and δ-valerolactone were found to be 106.1 and 110.7 kJ/mol, respectively. That is, although the $\Delta G^{\ddagger}$ value for *rac*-lactide was the same as for the homopolymerization process, the $\Delta G^{\ddagger}$ for δ-valerolactone increased in the presence of *rac*-lactide. The monomer reactivity ratios for this copolymerization reaction were determined from a Fineman–Ross plot which revealed that the polymer lactide unit favored ring-opening lactide monomer over δ-valerolactone thereby resulting in a tapered polylactide-polyvalerolactone copolymer.

EXPERIMENTAL SECTION

Methods and Materials. All manipulations were carried out using a double manifold Schlenk vacuum line under an argon atmosphere or an argon filled glovebox unless otherwise stated. Toluene was freshly distilled from sodium/benzophenone before use. Methanol and dichloromethane were purified by an MBraun Manual Solvent Purification System packed with Alcoa F200 activated alumina desiccant. Pentane was freshly distilled from CaH_2. Deuterated chloroform, deuterated benzene, and deuterated toluene from Cambridge Isotope Laboratories Inc. were stored in the glovebox and used as received. L-, D-lactide, and *rac*-lactide were gifts from PURAC America Inc. These lactides were recrystallized from toluene, dried under vacuum at 40 °C overnight, and

dx.doi.org/10.1021/ic2008057 |*Inorg. Chem.* 2011, 50, 6775–6787

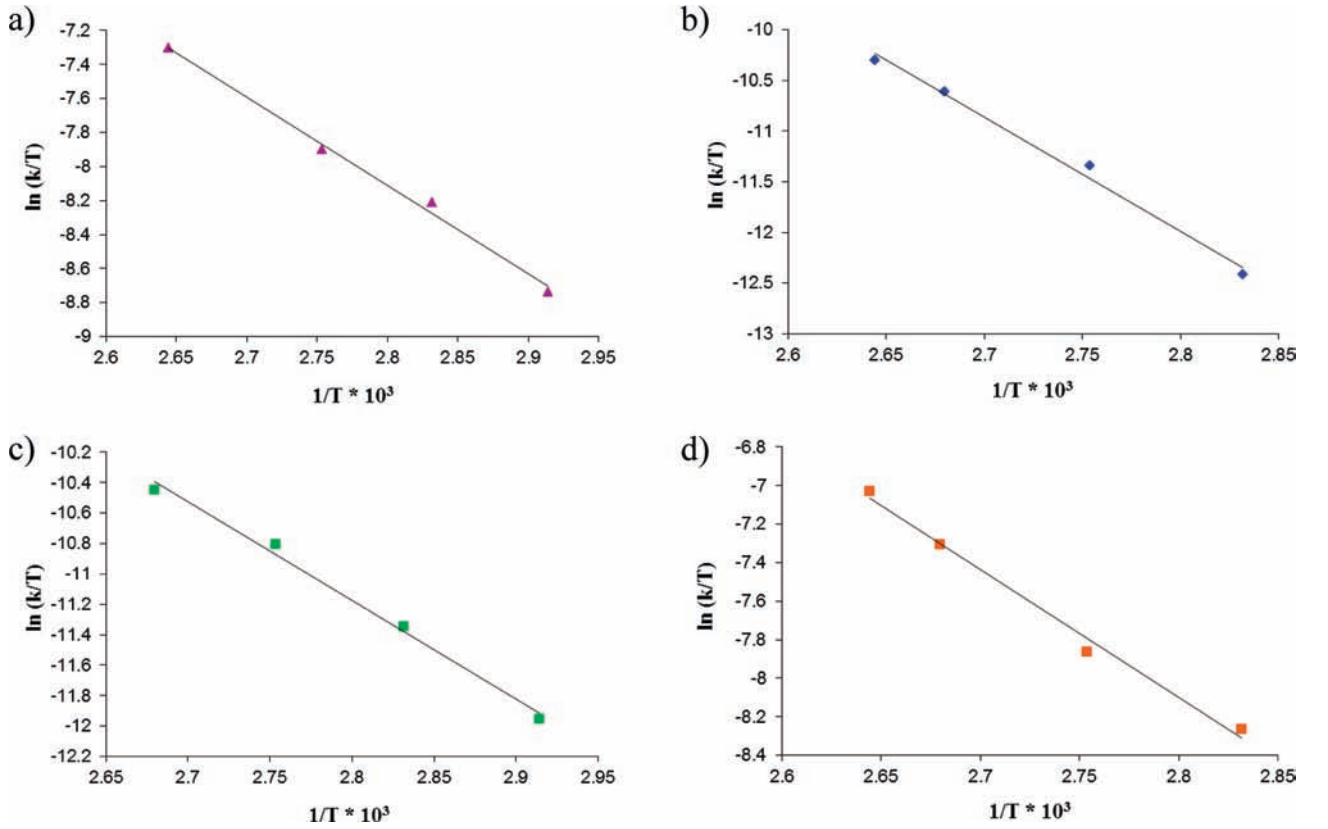

Figure 11. Eyring plot of ROP of (a) TMC (Slope = −5.193 with R^2 = 0.994), (b) *rac*-β-BL (Slope = −11.285 with R^2 = 0.990), (c) δ-VL (Slope = −6.500 with R^2 = 0.992), and (d) ε-CL (Slope = −6.645 with R^2 = 0.991) in the presence of catalyst **2g** in toluene-d_8.

Table 8. Activation Parameter in Homopolymerization of Cyclic Monomers at 90 °C

entry	monomer	k (mM^{-1} h^{-1})	$\Delta H^{\ddagger}$ (kJ/mol)	$\Delta S^{\ddagger}$ (J/mol K)	$\Delta G^{\ddagger}$ (kJ/mol)
1	*rac*-lactide	0.0111	59.7 ± 2.8	−129.1 ± 7.7	106.6
2	TMC	0.395	43.1 ± 2.2	−144.1 ± 6.3	95.4
3	*rac*-β-BL	0.0133	93.8 ± 6.3	−34.5 ± 17.1	106.3
4	δ-VL	0.0165	54.0 ± 3.3	−139.1 ± 9.3	104.5
5	ε-CL	0.331	55.2 ± 3.6	−110.2 ± 9.8	95.2

Table 9. Data Set of Mole Fraction of the Fineman−Ross Plot[a]

entry	*rac*-lactide: δ-valerolactone in the feed	F^b	*rac*-lactide: δ-valerolactone in the copolymer[c]	f^d
1	29:71	2.44	7.96:2.34	0.305
2	34:66	1.94	6.81:1.86	0.273
3	44:56	1.27	6.50:1.74	0.268
4	49:51	1.04	6.69:1.56	0.233
7	53:47	0.88	8.11:1.66	0.204

[a] Polymerization conditions: *rac*-lactide + δ-VL (818 μmol), ([*rac*-lactide]/[δ-VL])/[Al] = 100, in toluene-d_8 at 90 °C. [b] Mole fraction of δ-VL in the feed ($F = X_{VL,\ monomer}/X_{LA,\ monomer}$). [c] Determined by ^{1}H NMR. [d] Mole fraction of δ-VL in the polymer ($f = X_{VL,\ polymer}/X_{LA,\ polymer}$).

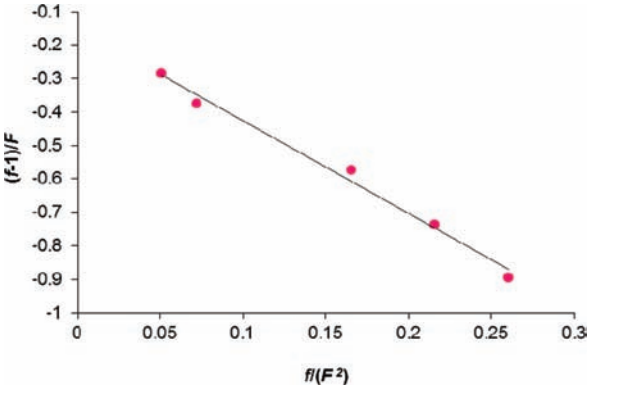

Figure 12. Plot of $(f-1)/F$ versus f/F^2 with slope = 2.78 and R^2 = 0.98, intercept = 0.14.

stored in the glovebox. β-butyrolactone, γ-butyrolactone, δ-valerolactone, and ε-caprolactone were distilled under vacuum from CaH_2 and stored in the glovebox. Trimethylene carbonate (Boehringer Ingelheim) was recrystallized from tetrahydrofuran and diethyl ether, dried under vacuo, and stored in the glovebox. 4-Amino-1-butanol and triethylaluminium were purchased from TCI America and Sigma-Aldrich, respectively, and used without further purification. Ethanolamine, 3-amino-1-propanol, 5-amino-1-pentanol, *trans*-2-aminocyclohexanol hydrochloride, 2-hydroxy-3-methoxybenzaldehyde, *rac*-methionine, *rac*-phenylalanine, and *tert*-butyldimethylchlorosilane were purchased from Alfa Aesar and used as received. 3,5-Di-*tert*-butyl-2-hydroxybenzaldehyde, 3-(*tert*-butyldimethylsilyl)-2-hydroxy-5-methylbenzaldehyde, and 2-hydroxy-5-methyl-3-(triphenylsilyl)benzaldehyde were prepared according to a published procedure.[27] All other compounds and reagents were obtained from Sigma-Aldrich and were used without further purification. The preparation and spectral

dx.doi.org/10.1021/ic2008057 |*Inorg. Chem.* 2011, 50, 6775–6787

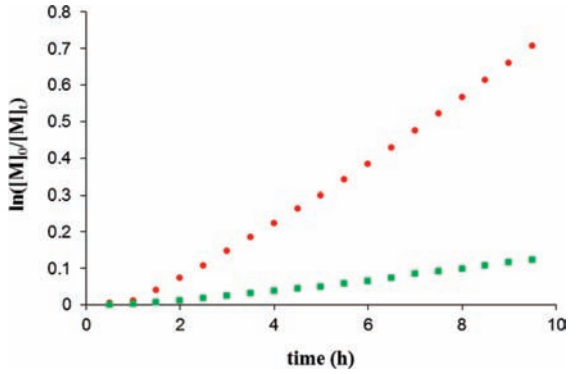

Figure 13. Plot of $\ln([M]_0/[M]_t)$ vs time depicting a reaction order of unity with respect to *rac*-lactide (red solid circles) and δ-VL (green solid squares) concentration (R^2 = 0.993 for polylactide and R^2 = 0.991 for poly-δ-VL).

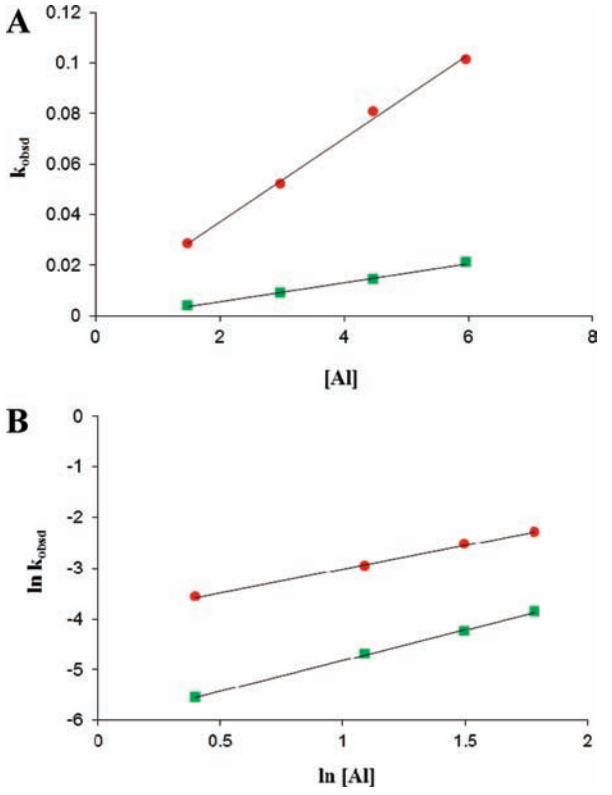

Figure 14. (**A**) Plot of k_{obsd} vs [Al] with slope = 0.016 for *rac*-lactide (red solid circles, R^2 = 0.996) and slope = 0.038 for δ-VL(green solid squares, R^2 = 0.995). (**B**) Plot of ln k_{obsd} vs ln[Al] with slope =0.92 for *rac*-lactide (red solid circles, R^2 = 0.997) and slope = 1.20 for δ-VL(green solid squares, R^2 = 0.999).

characterization of all ligands and their aluminum complexes have previously been reported in detail in an earlier publication.[12] Analytical elemental analysis was provided by Canadian Microanalytical Services Ltd.

Measurements. ^{1}H NMR spectra were recorded on Unity+ 300 or 500 MHz and VXR 300 or 500 MHz superconducting NMR spectrometers. Molecular weight determinations were carried out with Viscotek Modular GPC apparatus equipped with ViscoGEL I-series columns (H + L) and Model 270 dual detector composed of refractive index and light scattering detectors. DSC measurements were performed with a Polymer DSC by Mettler Toledo. The samples were scanned from −100 to 200 °C under nitrogen atmosphere. The glass transition temperature (T_g) was determined from the second heating at a heating rate of 5 °C/min. X-ray crystallography was done on a Bruker GADDS X-ray diffractometer in a nitrogen cold stream maintained at 110 K.

Table 10. Rate Constants Dependence on the Concentration of the Catalyst (2g) and Temperature in Copolymerization of *rac*-Lactide and δ-valerolactone[a]

entry	[Al] (mM)	temp (°C)	k_{obsd} (h^{-1})	k_{obsd}(h^{-1})
1	1.49	90	0.0285	0.0039
2	2.98	90	0.0520	0.0091
3	4.47	90	0.0808	0.0143
4	5.96	90	0.101	0.0211
5	4.47	80	0.0379	0.0061
6	4.47	100	0.147	0.0345
7	4.47	105	0.194	0.0425

[a] Monomer concentration was held constant at 0.69 M and reactions carried out in toluene-d_8. The feed ratio of monomers was 1:1.

Table 11. Comparison of Rates and Activation Parameters in Homopolymerization and Copolymerization of *rac*-lactide and δ-VL Catalyzed by Complex 2g

	homopolymerization		copolymerization	
	rac-lactide	δ-VL	*rac*-lactide	δ-VL
$\Delta H^{\ddagger}$ (kJ/mol)	59.7 ± 2.8	54.0 ± 3.3	69.7 ± 2.5	85.7 ± 4.9
$\Delta S^{\ddagger}$ (J/mol K)	−129.1 ± 7.7	−139.1 ± 9.3	−100.2 ± 6.9	−68.8 ± 13.3
$\Delta G^{\ddagger}$ (kJ/mol)[a]	106.6	104.5	106.1	110.7

[a] Free energy of activated calculated at 90 °C.

Lactide Polymerization Procedure. In a typical experiment carried out in the argon filled glovebox a Teflon-screw-capped heavy walled pressure vessel containing the corresponding aluminum complex (**2a**−**k**) and 50 equiv of *rac*-lactide (per aluminum center) in 1.00 mL of toluene was stirred at 70 °C for the designated time period. Upon removal of a small sample of the crude product via syringe, it was analyzed by ^{1}H NMR spectroscopy in $CDCl_3$. The product was isolated and purified by precipitation from dichloromethane by the addition of 5% hydrochloric acid in methanol. The solid polymer was collected and dried under vacuum to constant weight.

Kinetic Studies for Homopolymers. In a typical experiment carried out in the argon filled glovebox (Table 3, entry 3), a J. Young NMR tube containing 0.41 mmol of an appropriate monomer (*rac*-lactide, trimethylene carbonate (TMC), β-butyrolactone, γ-butyrolactone, δ-valorolactone, or ε-caprolactone) was added 0.1 mL of complex **2g** in deuterated toluene from a 8.94 mM stock solution. Next, 0.5 mL of deuterated toluene was added to adjust the total volume to 0.6 mL. The NMR tube was then placed to the preheated NMR spectrometer at corresponding temperature (70−105 °C, typically 90 °C), and the % conversion was investigated from the integration of polymer and monomer signals. The characteristic chemical shift for each monomer in deuterated toluene is 4.12 (q, −CH−; lactide), 3.62(m, −CH_2−; TMC), 3.93 (m, −CH−; β-butyrolactone), 3.63 (t, −CH_2−; δ-valerolactone), and 3.63 (m, −CH_2−; ε-caprolactone). The characteristic chemical shif for each polymer in deuterated toluene is 5.12 (q, −CH−; polylactide), 4.06(t, −CH_2−; TMC), 5.31 (m, −CH−; poly-β-butyrolactone), 3.95 (t, −CH_2−; poly-δ-valerolactone), and 4.00 (t, −CH_2−; poly-ε-caprolactone).

Kinetic Studies for Copolymers. In a typical experiment carried out in the argon filled glovebox (Table 10, entry 3), a J. Young NMR tube containing 0.41 mmol of *rac*-lactide and 0.41 mmol of δ-VL was

dx.doi.org/10.1021/ic2008057 |*Inorg. Chem.* 2011, 50, 6775–6787

added 0.1 mL of complex **2g** in deuterated toluene from a 8.94 mM stock solution. Next, 0.5 mL of deuterated toluene was added to adjust the total volume to 0.6 mL. The NMR tube was then placed to the preheated NMR spectrometer at corresponding temperature (70−105 °C, typically 90 °C), and the % conversion was investigated from the integration of polymer and monomer signals.

■ ASSOCIATED CONTENT

Supporting Information. Tables and CIF files giving crystallographic data for all complexes reported in this study. This material is available free of charge via the Internet at http://pubs.acs.org.

■ AUTHOR INFORMATION

Corresponding Author

*E-mail: djdarens@mail.chem.tamu.edu.

■ ACKNOWLEDGMENT

We gratefully acknowledge the financial support of the National Science Foundation (CHE-05-43133) and the Robert A. Welch Foundation (A-0923). We also thank Dr. Gina M. Chiarella for help solving structure **4e**. We also thank PURAC America, Inc. for providing lactide samples for this research. This research was also supported in part by an award from the Department of Energy (DOE) Office of Science Graduate Fellowship Program (DOE SCGF). The DOE SCGF Program was made possible in part by the American Recovery and Reinvestment Act of 2009. The DOE SCGF program is administered by the Oak Ridge Institute for Science and Education for the DOE. ORISE is managed by Oak Ridge Associated Universities (ORAU) under DOE contract number DE-AC05-06OR23100. All opinions expressed in this paper are the author's and do not necessarily reflect the policies and views of DOE, ORAU, or ORISE.

■ REFERENCES

(1) Williams, C. K.; Hillmyer, M. A. *Polym. Rev.* **2008**, *48*, 1–10.

(2) (a) Schmack, G.; Tändler, B.; Vogel, R.; Beyreuther, R.; Jacobsen, S.; Fritz, H. G. *J. Appl. Polym. Sci.* **1999**, *73*, 2785–2797. (b) Perepelkin, K. E. *Fibre Chem.* **2002**, *34*, 85–100. (c) Avinc, O.; Khoddami, A. *Fibre Chem.* **2009**, *41*, 391–401.

(3) (a) Paulsson, M.; Singh, S. K. *J. Pharm. Sci.* **1999**, *88*, 406–411. (b) Uhrich, K. E.; Cannizzaro, S. M.; Langer, R. S.; Shakesheff, K. M. *Chem. Rev.* **1999**, *99*, 3181–3198.

(4) (a) Penco, M.; Donetti, R.; Mendichi, R.; Ferruti, P. *Macromol. Chem. Phys.* **1998**, *199*, 1737–1745. (b) Ikada, Y.; Tsuji, H. *Macromol. Rapid Commun.* **2000**, *21*, 117–132. (c) Platel, R. H.; Hodgson, L. M.; Williams, C. K. *Polym. Rev.* **2008**, *48*, 11–63.

(5) Reichardt, R.; Vagin, S.; Reithmeier, R.; Ott, A. K.; Rieger, B. *Macromolecules* **2010**, *43*, 9311–9317.

(6) Dobroth, Z. T.; Hu, S.; Coats, E. R.; McDonald, A. G. *Bioresour. Technol.* **2011**, *102*, 3352–3359.

(7) van der Walle, G.; de Koning, G.; Weusthuis, R.; Eggink, G. In *Biopolyesters*; Babel, W., Steinbüchel, A., Eds.; Springer: Berlin/Heidelberg: 2001; Vol. 71, pp 263−291.

(8) Tabone, M. D.; Cregg, J. J.; Beckman, E. J.; Landis, A. E. *Environ. Sci. Technol.* **2010**, *44*, 8264–8269.

(9) Toncheva, N.; Jerome, R.; Mateva, R. *Eur. Polym. J.* **2011**, *47*, 238–247.

(10) Jansen, J.; Bosman, M. B.; Boerakker, M. J.; Feijen, J.; Grijpma, D. W. *J. Controlled Release* **2010**, *148*, e79–e80.

(11) Ghosh, S. *J. Chem. Res.* **2004**, *4*, 241–246.

(12) Darensbourg, D. J.; Karroonnirun, O. *Organometallics* **2010**, *29*, 5627–5634.

(13) The M_n values for polylactide were corrected from the M_n values determined by GPC vs polystyrene standards, as previously reported in the literature. (a) Barak, I.; Dubois, P.; Jérôme, R.; Teyssié, Ph. *J. Polym. Sci., Part A: Polym. Chem.* **1993**, *31*, 305. (b) Baran, J.; Duda, A.; Kowalski, A.; Szymanski, R.; Penczek, S. *Macromol. Rapid Commun.* **1997**, *18*, 325–333.

(14) (a) Hormnirun, P.; Marshall, E. L.; Gibson, V. C.; White, A. J. P.; Williams, D. J. *J. Am. Chem. Soc.* **2004**, *126*, 2688–2689. (b) Nomura, N.; Ishii, R.; Yamamoto, Y.; Kondo, T. *Chem.—Eur. J.* **2007**, *13*, 4433–4451.

(15) Zhang, L.; Nederberg, F.; Messman, J. M.; Pratt, R. C.; Hedrick, J. L.; Wade, C. G. *J. Am. Chem. Soc.* **2007**, *129*, 12610–12611.

(16) (a) Nomura, N.; Ishii, R.; Akakura, M.; Aoi, K. *J. Am. Chem. Soc.* **2002**, *124*, 5938–5939. (b) Ovitt, T. M.; Coates, G. W. *J. Am. Chem. Soc.* **2002**, *124*, 1316–1326.

(17) (a) Chisholm, M. H.; Patmore, N. J.; Zhou, Z. *Chem. Commun.* **2005**, 127–129. (b) Chisholm, M. H.; Gallucci, J. C.; Quisenberry, K. T.; Zhou, Z. *Inorg. Chem.* **2008**, *47*, 2613–2624.

(18) Brookhart, M.; Grant, B.; Volpe, A. F. *Organometallics* **1992**, *11*, 3920–3922.

(19) (a) Adams, J. *Acta Crystallogr., Sect. B* **1979**, *35*, 1084–1088. (b) Valle, G. C.; Bombi, G. G.; Corain, B.; Favarato, M.; Zatta, P. *J. Chem. Soc., Dalton Trans.* **1989**, 1513–1517. (c) Mason, M. R.; Smith, J. M.; Bott, S. G.; Barron, A. R. *J. Am. Chem. Soc.* **1993**, *115*, 4971–4984. (d) Schnitter, C.; Roesky, H. W.; Albers, T.; Schmidt, H.-G.; Röpken, C.; Parisini, E.; Sheldrick, G. M. *Chem.—Eur. J.* **1997**, *3*, 1783–1792. (e) Veith, M.; Jarczyk, M.; Huch, V. *Angew. Chem., Int. Ed.* **1998**, *37*, 105–108. (f) Chen, H.-L.; Ko, B.-T.; Huang, B.-H.; Lin, C.-C. *Organometallics* **2001**, *20*, 5076–5083. (g) Zhu, H.; Chai, J.; He, C.; Bai, G.; Roesky, H. W.; Jancik, V.; Schmidt, H.-G.; Noltemeyer, M. *Organometallics* **2004**, *24*, 380–384. (h) Joszai, R.; Kerekes, I.; Satoshi, I.; Sawada, K.; Zekany, L.; Toth, I. *Dalton Trans.* **2006**, 3221–3227. (i) Li, X.; Song, H.; Duan, L.; Cui, C.; Roesky, H. W. *Inorg. Chem.* **2006**, *45*, 1912–1914. (j) Cametti, M.; Dalla Cort, A.; Colapietro, M.; Portalone, G.; Russo, L.; Rissanen, K. *Inorg. Chem.* **2007**, *46*, 9057–9059.

(20) Alemán, C.; Betran, O.; Casanovas, J.; Houk, K. N.; Hall, H. K. *J. Org. Chem.* **2009**, *74*, 6237–6244.

(21) Rieth, L. R.; Moore, D. R.; Lobkovsky, E. B.; Coates, G. W. *J. Am. Chem. Soc.* **2002**, *124*, 15239–15248.

(22) Ouhadi, T.; Hamitou, A.; Jerome, R.; Teyssie, P. *Macromolecules* **1976**, *9*, 927–931. Dubois, P.; Jacobs, C.; Jerome, R.; Teyssie, P. *Macromolecules* **1991**, *24*, 2266–2270. Biela, T.; Duda, A.; Penczek, S. *Polym. Prepr. (Am. Chem. Soc., Div. Polym. Chem.)* **1994**, *35*, 508–509.

(23) Chamberlain, B. M.; Jazdzewski, B. A.; Pink, M.; Hillmyer, M. A.; Tolman, W. B. *Macromolecules* **2000**, *33*, 3970–3977.

(24) Duda, A.; Penczek, S. *Macromol. Rapid Commun.* **1994**, *15*, 559–566.

(25) Fineman, M.; Ross, S. D. *J. Polym. Sci.* **1950**, *5*, 259–262.

(26) Coulembier, O.; Degée, P.; Hedrick, J. L.; Dubois, P. *Prog. Polym. Sci.* **2006**, *31*, 723–747.

(27) Hansen, T. V.; Skattebøl, L. *Tetrahedron Lett.* **2005**, *46*, 3829–3830. Darensbourg, D. J.; Choi, W.; Richers, C. P. *Macromolecules* **2007**, *40*, 3521–3523. Thadani, A. N.; Huang, Y.; Rawal, V. H. *Org. Lett.* **2007**, *9*, 3873–3876. Darensbourg, D. J.; Choi, W.; Karroonnirun, O.; Bhuvanesh, N. *Macromolecules* **2008**, *41*, 3493–3502.